REPORT DOCUMENTATION PAGE

Form Approved OMB NO. 0704-0188

1. REPORT DATE (DD-MM-YYYY)	2. REPORT TYPE	3. DATES COVERED (From - To)
14-11-2014	Final Report	1-Aug-2013 - 31-Jul-2014

4. TITLE AND SUBTITLE
FINAL REPORT for W911NF-13-1-0333
Thermal: Differential Scanning Calorimetry (DSC), Thermogravimetric Analysis (TGA), and Polarized Microscopy Instrumentation for the Analysis of Field-Controlled Anisotropic Nanomaterials

5a. CONTRACT NUMBER
W911NF-13-1-0333

5b. GRANT NUMBER

5c. PROGRAM ELEMENT NUMBER
611103

6. AUTHORS
Philip A. Sullivan, Ph.D.

5d. PROJECT NUMBER

5e. TASK NUMBER

5f. WORK UNIT NUMBER

7. PERFORMING ORGANIZATION NAMES AND ADDRESSES
Montana State University
309 Montana Hall
Box 172470
Bozeman, MT 59717 -2470

8. PERFORMING ORGANIZATION REPORT NUMBER

9. SPONSORING/MONITORING AGENCY NAME(S) AND ADDRESS (ES)
U.S. Army Research Office
P.O. Box 12211
Research Triangle Park, NC 27709-2211

10. SPONSOR/MONITOR'S ACRONYM(S)
ARO

11. SPONSOR/MONITOR'S REPORT NUMBER(S)
63476-CH-RIP.2

12. DISTRIBUTION AVAILIBILITY STATEMENT
Approved for Public Release; Distribution Unlimited

13. SUPPLEMENTARY NOTES
The views, opinions and/or findings contained in this report are those of the author(s) and should not contrued as an official Department of the Army position, policy or decision, unless so designated by other documentation.

14. ABSTRACT
Montana State University, Bozeman, (MSU) is quite well equipped for cutting-edge chemistry and materials science research in many areas of interest to the DoD. However, although the need is great, MSU did not previously own thermal/thermo-optical characterization equipment. In order to enable detailed investigation of the thermal properties of complex materials, funding for the acquisition of a complementary suite of thermal and optical measurement instruments was awarded to Montana State University. A TA Instruments Discovery Series Differential Scanning Calorimeter (DSC), a TA Instruments Discovery Series Thermogravimetric Analyzer (TGA)

15. SUBJECT TERMS
Thermal Analysis, Differential Scanning Calorimetry, Thermogravimetric Analysis, Nanomaterials, Metamaterials

16. SECURITY CLASSIFICATION OF:			17. LIMITATION OF ABSTRACT	15. NUMBER OF PAGES	19a. NAME OF RESPONSIBLE PERSON
a. REPORT	b. ABSTRACT	c. THIS PAGE			Philip Sullivan
UU	UU	UU	UU		19b. TELEPHONE NUMBER 406-994-5692

Report Title

FINAL REPORT for W911NF-13-1-0333
Thermal: Differential Scanning Calorimetry (DSC), Thermogravimetric Analysis (TGA), and Polarized Microscopy Instrumentation for the Analysis of Field-Controlled Anisotropic Nanomaterials

ABSTRACT

Montana State University, Bozeman, (MSU) is quite well equipped for cutting-edge chemistry and materials science research in many areas of interest to the DoD. However, although the need is great, MSU did not previously own thermal/thermo-optical characterization equipment. In order to enable detailed investigation of the thermal properties of complex materials, funding for the acquisition of a complementary suite of thermal and optical measurement instruments was awarded to Montana State University. A TA Instruments Discovery Series Differential Scanning Calorimeter (DSC), a TA Instruments Discovery Series Thermogravimetric Analyzer (TGA), and an Olympus BX51 Polarized Light Microscope (PLM) were purchased and installed using the funding provided. This equipment is currently benefiting several ongoing research projects with potential benefit to the DoD.

Enter List of papers submitted or published that acknowledge ARO support from the start of the project to the date of this printing. List the papers, including journal references, in the following categories:

(a) Papers published in peer-reviewed journals (N/A for none)

Received		Paper
11/14/2014	1.00	Alec Rose, Ryan Latterman, David R. Smith, Philip Sullivan. Lower poling thresholds and enhanced Pockels coefficients in nanoparticle-polymer composites, Applied Physics Letters, (07 2013): 31102. doi: 10.1063/1.4813751
TOTAL:	**1**	

Number of Papers published in peer-reviewed journals:

(b) Papers published in non-peer-reviewed journals (N/A for none)

Received		Paper
TOTAL:		

Number of Papers published in non peer-reviewed journals:

(c) Presentations

Number of Presentations: 0.00

Non Peer-Reviewed Conference Proceeding publications (other than abstracts):

Received Paper

TOTAL:

Number of Non Peer-Reviewed Conference Proceeding publications (other than abstracts):

Peer-Reviewed Conference Proceeding publications (other than abstracts):

Received Paper

TOTAL:

Number of Peer-Reviewed Conference Proceeding publications (other than abstracts):

(d) Manuscripts

Received Paper

TOTAL:

Number of Manuscripts:

Books

Received Book

TOTAL:

Received	Book Chapter

TOTAL:

Patents Submitted

Patents Awarded

Awards

Graduate Students

NAME	PERCENT_SUPPORTED	Discipline
Not applicable (equiment purchase	0.00	
FTE Equivalent:	**0.00**	
Total Number:	**1**	

Names of Post Doctorates

NAME	PERCENT_SUPPORTED
Not Applicable (equipment purcha	0.00
FTE Equivalent:	**0.00**
Total Number:	**1**

Names of Faculty Supported

NAME	PERCENT_SUPPORTED	National Academy Member
Not Applicable (equipment purcha	0.00	
FTE Equivalent:	**0.00**	
Total Number:	**1**	

Names of Under Graduate students supported

NAME	PERCENT_SUPPORTED	Discipline
Not Apllicable (equipment purchas	0.00	
FTE Equivalent:	**0.00**	
Total Number:	**1**	

Student Metrics

This section only applies to graduating undergraduates supported by this agreement in this reporting period

The number of undergraduates funded by this agreement who graduated during this period: 0.00

The number of undergraduates funded by this agreement who graduated during this period with a degree in science, mathematics, engineering, or technology fields:..... 0.00

The number of undergraduates funded by your agreement who graduated during this period and will continue to pursue a graduate or Ph.D. degree in science, mathematics, engineering, or technology fields:..... 0.00

Number of graduating undergraduates who achieved a 3.5 GPA to 4.0 (4.0 max scale):..... 0.00

Number of graduating undergraduates funded by a DoD funded Center of Excellence grant for Education, Research and Engineering:..... 0.00

The number of undergraduates funded by your agreement who graduated during this period and intend to work for the Department of Defense 0.00

The number of undergraduates funded by your agreement who graduated during this period and will receive scholarships or fellowships for further studies in science, mathematics, engineering or technology fields: 0.00

Names of Personnel receiving masters degrees

NAME
Not Applicable (equipment purchase
Total Number: 1

Names of personnel receiving PHDs

NAME
Not Applicable (equipment purchase
Total Number: 1

Names of other research staff

NAME	PERCENT_SUPPORTED
FTE Equivalent:	
Total Number:	

Sub Contractors (DD882)

Inventions (DD882)

Scientific Progress

High-level theoretical analysis tools have been developed and employed in order to better understand the parameter space relevant to the design of hybrid organic/metal-nanoparticle meta-elements and –materials. The first results from this work were published recently in Applied Physics Letters 103, 031102 (2013). These data have been translated to guide the goals of material synthesis efforts. Materials synthesis to date has consisted of learning to prepare and modify nonlinear dyes, block copolymers, gold nanorods, and functionalized surfaces to yield desired optical/physical properties. Gold nanorods of various length/width aspect ratios (with correspondingly varied optical properties) have been successfully functionalized with multi-block copolymers and/or alkane-thiol functionalized ONLOs. Vertical nanorod (nanopillar) array samples from the Anatoly Zayats research lab at Kings College, London have also been functionalized with ONLOs and analyzed.(6) Nonlinear effects resulting from these efforts are being evaluated using Sum
Frequency Generation (SFG) and Second Harmonic Generation (SHG) in collaboration with Professor Robert Walker's Lab at MSU. Quite promising results have been realized through direct covalent attachment of alkane-thiol functionalized ONLOs within vertical nanorod arrays. SFG data confirms the existence of large Chi(2) without external symmetry breaking (electric field poling). Additionally, when these samples are compared with ONLOs attached to flat gold surfaces, using polarization resolved SFG, quite different nonlinear optical behavior is observed. Specifically, in the case of ONLO interspersed vertical nanorod array samples, orthogonally polarized visible (801 nm) and IR (3250 nm) optical inputs give rise to large SFG signals. In contrast only parallel polarized visible and IR inputs give rise to
significant SFG in the case of ONLOs attached to flat (unstructured) gold surfaces. These results are potentially very significant, proving that hybrid nanostructured NLMMs can yield large Chi (2) responses and suggesting that appropriately designed NLMMs may be used to introduce non-natural effective Chi(2) tensor elements. A publication detailing these results is currently in preparation. Work has also commenced toward the preparation of improved Chi(2) materials for nanocomponent integration (section 2.3 of proposal number 62059-CH). This work seeks to explore the preparation of selected pendant modified ONLO chromophores (PMCs) in order to yield materials with
improved (or entirely spontaneous) long-range acentric organization. Such acentric organization will yield improved Chi(2) values that may be directly incorporated into nanostructured hybrid NLMMs. So far, rigid body Monte Carlo computer simulations have been performed to guide PMC structure selection (in collaboration with Professor Bruce H. Robinson at University of Washington). Based on computer simulation results, several new PMC structures have been selected and prepared in our labs at MSU. New chemical methods were
developed to enable their preparation. Physical, chemical, and nonlinear optical property analyses are currently underway.The new Instrumentation purchased under W911NF-13-1-0333 has been critical to the efforts detailed above as well as other ongoing research efforts at MSU. For example: Professor Paul Gannon (MSU Chemical and Biological Engineering Department, and director of the MSU High-Temperature Materials Laboratory) and others are currently exploring high-temperature corrosion and corrosion reduction.This research is of primary interest for protection of materials used in turbine engines, and similar systems. The DSC/TGA systems purchased with the awarded funds are being used to simulate high-temperature combustion environments, while precisely measuring test specimen mass and indicating critical phase changes as a function of environmental exposure.

Technology Transfer

FINAL REPORT for W911NF-13-1-0333
Thermal: Differential Scanning Calorimetry (DSC), Thermogravimetric Analysis (TGA), and Polarized Microscopy Instrumentation for the Analysis of Field-Controlled Anisotropic Nanomaterials

ARO DURIP: FY13
PA-AFOSR-2012-0004

- **Principle Investigator:** Philip A. Sullivan, *Phone:* 406-994-5692, *Fax:* 406-994-5407,
  e-mail: psullivan@chemistry.montana.edu

- **Institution address:** Montana State University
  Department of Chemistry and Biochemistry
  103 Chemistry and Biochemistry Building, Bozeman, MT 59717-2470

- **Current DoD Contractor or Grantee:** YES

- **Institution Proposal Number:** 413-1180

- **Administrative/business contact:** Traci Miyakawa, Senior Fiscal Manager, Montana State University, Office of Sponsored Programs, 309 Montana Hall, Bozeman, MT 59717-2470, *Phone:* 406-994-7696, *Fax:* 406-994-7951, *e-mail:* tracim@montana.edu

- **Start Date: 08/01/2013**

- **End Date: 07/31/2014**

Table of contents:

Executive Summary:

In order to enable detailed investigation of the thermal properties of complex materials, funding for the acquisition of a complementary suite of thermal and optical measurement instruments was awarded to Montana State University. A TA Instruments Discovery Series Differential Scanning Calorimeter (DSC), a TA Instruments Discovery Series Thermogravimetric Analyzer (TGA), and an Olympus BX51 Polarized Light Microscope (PLM) were purchased and installed using the funding provided. The quoted price for the DSC plus TGA system (see sections 1.1 and 1.2) is $224,155.00. However, TA Instruments has extended a "Buy 1 Get 1 Free" offer. The total discount received was - $92,600.00, reducing the system (DSC & TGA) total to $131,555.00. The purchase price for the complete Olympus BX51 PLM system, as outlined in section 1.3, was $37,248.00. The total dollar amount funded for the purchase of the DSC, TGA, and PLM was: $168,803.00.

Montana State University, Bozeman, (MSU) is quite well equipped for cutting-edge chemistry and materials science research in many areas of interest to the DoD. However, although the need is great, MSU did not previously own thermal/thermo-optical characterization equipment with capabilities comparable to that purchased with the funds provided here. DoD currently funds ongoing materials science research in several MSU departments that are benefiting greatly from the capabilities that the equipment purchased here provides (see sections 2 and 3). For example, the Sullivan Lab in the MSU Chemistry and Biochemistry Department is pursuing a research program, funded by the Army Research Office (Sullivan ARO # W911NF-12-1-0333) focusing on the nonlinear optical properties of anisotropic hybrid organic/metal nanoparticle photonic materials (nonlinear metamaterials). Several projects in MSU engineering are currently funded by an ONR MURI (grant # N00014-10-1-0946) to explore the biocorrosion of carbon steel and fuels that are exposed to seawater. The goal of this research is to predict, diagnose and mitigate fuel biodeterioration and biocorrosion problems impacting US Navy operations. Professor Paul Gannon (MSU Chemical and Biological Engineering Department, and director of the MSU High-Temperature Materials Laboratory) and others are currently exploring high-temperature corrosion and corrosion reduction. This research is of primary interest for protection of materials used in turbine engines, and similar systems. The DSC/TGA systems purchased through this award are currently being used to simulate high-temperature combustion environments, while precisely measuring test specimen mass and indicating critical phase changes as a function of environmental exposure. Professor Steven Sophie, an assistant professor of the MSU Department of Mechanical and Industrial Engineering, is developing new anode technologies for high-temperature electro-chemical power generation as well as high-temperature electrolysis (see letter attached). High-temperature stability may be improved by the fabrication of mixed conducting double perovskite materials as well as the thermal stabilization of nickel catalyst nano-particles. New double perovskites being synthesized at MSU need to be characterized for chemical and structural uniformity as well as thermal properties. Professor Trevor Douglas, of the MSU Chemistry and Biochemistry Department, and director of the MSU Center for Bioinspired Nanomaterials, has pioneered the use of viruses (virus capsids) as supramolecular platforms for synthetic manipulation with a range of applications from materials to medicine. Optical and thermal characterization of these materials and assemblies thereof will provide much needed information about material structural transitions in the protein cage architecture, and the material encapsulated within the capsid.

The equipment purchased with funds provided by this award are currently housed in the MSU Chemistry and Biochemistry Department, in dedicated space, and are being overseen and

maintained by Professor Philip A. Sullivan. Access to the instrumentation is being provided to users across campus in order to augment exisiting research capabilities.

1. Instrument Descriptions

1.1. Differential Scanning Calorimeter (DSC). DSC has been refined and optimized over the course of more than 4 decades and emerged as a powerful materials science analytical technique.(1, 2) In DSC analysis, a differential scanning calorimeter is used to measure heat flux vs. temperature and/or time. A sample and an inert reference are simultaneously heated or cooled at a chosen linear rate while the difference in heat flow between them is monitored. The resulting differential heat flow data are then plotted vs. temperature or time. A positive or negative change in this differential reveals the occurrence of a thermally enabled endothermic or exothermic process such as a phase transition or chemical reaction. Accurate and sensitive DSC measurements allow quantitative characterization of bulk material thermal transitions such as glass transition, fusion, crystallization, and melting. Chemical reactions such as thermal- or photo-polymerization (curing), and oxidation may also be easily investigated using DSC.

$$\Delta H = KA \qquad \text{(eq. 1)}$$

Enthalpies of transition, ΔH, may easily be calculated from a DSC plot using equation 1. Here K is the calorimetric constant, determined for each instrument using a calibration standard (e.g., indium), and A is the area under the response curve.

1.1.1 Instrument Overview: TA Instruments Discovery Series DSC (modulated DSC). TA Instruments installed their new Discovery Series line of thermal analysis instrumentation.(3) The discovery series DSC offers best-available sensitivity, resolution, and reproducibility. TA Instruments is a U.S. company and a leading manufacturer of thermal analysis instruments worldwide.

Figure 1.1.1: The TA instruments Discovery Series DSC system (left). The Discovery Series DSC furnace compartment showing the transducer and new diffusion bonded sensor (right).

Several design improvements contribute to the enhanced sensitivity, resolution and baseline linearity/repeatability (±5μW) of the Discovery Series instruments. The Discovery series DSC boasts an industry leading indium response ratio of ≥ 90 approximately a five-fold improvement over the comparable quality Perkin Elmer 8000 series instruments (reported response ratio of ~ 18).

$$\Delta Q = \frac{T_{sample} - T_{ref} + A + B + C}{R} \approx \frac{\Delta T}{R} \qquad \text{(eq. 2)}$$

TA Instruments has trademarked the combination of these improvements as Tzero™ Technology. A simplified explanation of these improvements and their effects can be given by first examining

the basic equation governing DSC heat flow analysis (equation 2). In equation 2, Q denotes heat flow, where the time dependent change in this quantity, ΔQ, is defined as the difference in temperature, ΔT, between the sample and reference (T_{sample}-T_{ref}) divided by the thermal resistance between the sample, reference, and furnace. The parameters A, B, and C, represent thermal resistance, thermal capacitance, and heating rate imbalances, respectively. If no such imbalances exist between sample-furnace, reference-furnace, and sample-reference, A, B, and C are zero, and ΔQ is simply ΔT/R. In most conventional DSC designs T_{sample} and $T_{reference}$ are measured relative to furnace temperature using two thermocouples (one on each sample transducer). In this design, A, B, and C are neglected (not directly measured). Neglecting these imbalances leads to performance limitations that are related to uncompensated thermal lag between sample and measurement elements.

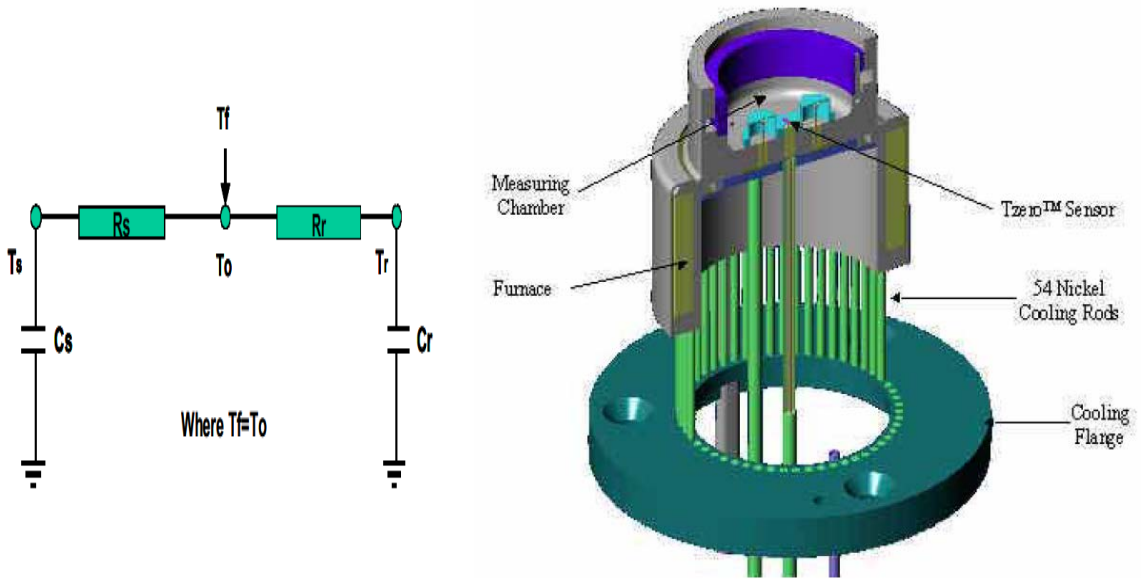

Figure 1.1.2: Schematic of the Tzero™ cell design showing the third (Tzero™) reference thermocouple (left). The Discovery Series DSC furnace is placed directly below the transducer stage and coupled through a machined silver block (right).

Tzero™ technology employs a third (reference) transducer thermocouple that is placed directly between the furnace and transducer stage (figure 1.1.2, right). This reference transducer measures T_0, which is essentially the same as the furnace temperature, T_f. Because of it's location, heat flows through the Tzero™ thermocouple to each of the samples, allowing T_0 to be used as a direct reference point for heat flow to T_{sample} and T_{ref}. A thermal circuit diagram of this design is shown in figure 1.1.2 (left). The Tzero™ design allows virtually complete compensation for A, B, and C in equation 2, effectively eliminating errors related to thermal imbalances and lag. This compensation capability reduces response peak-shape distortion, improving both sensitivity (the magnitude of response/sample weight) and resolution (full width of response peak at half maximum), and yielding an industry leading response ratio (ratio of the two).(3)

In addition to improvements in traditional DSC analysis capabilities, the Discovery Series DSC also offers modulated DSC (MDSC) analysis as a standard feature that can be selected or deselected by the end user. MDSC analysis allows deconvolution of simultaneously occurring changes in heat capacity and kinetic events. The MDSC technique involves the use of two simultaneous heating/cooling rates (figure 1.1.3, left). A sinusoidal temperature modulation is superimposed on the traditional DSC heating/cooling ramp rate as shown in figure 1.1.3.

$$\frac{dH}{dt} = Cp\frac{dT}{dt} + f(T,t) \qquad \text{(eq.3)}$$

The heat flow data derived from MDSC can be described using equation 3. Here, dH/dt represents the total heat flow corresponding to the linear heating rate. Cp*(dT/dt) is the reversing heat flow component derived from the magnitude of heat flow that responds to sinusoidal modulation.

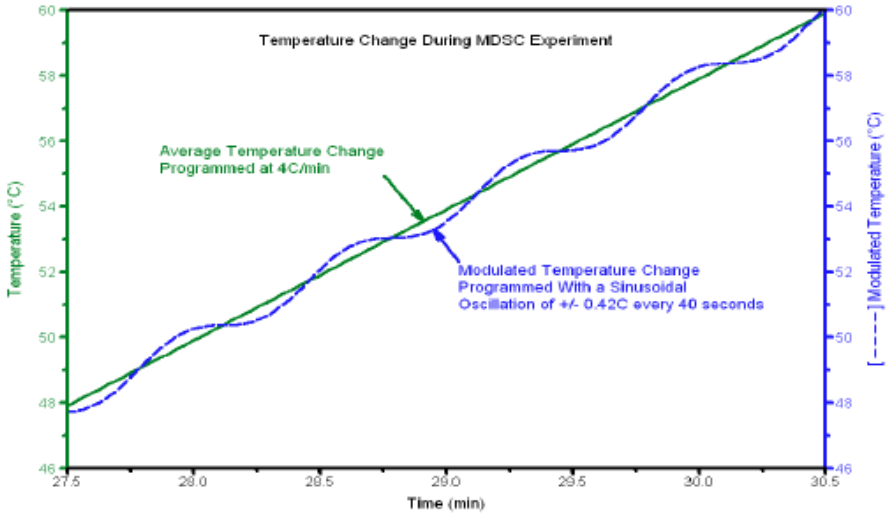

Figure 1.1.3: Modulated DSC (MDSC) temperature ramp profile. A sinusoidal thermal modulation is superimposed on the standard linear temperature ramp allowing simultaneous analysis of reversing (changes in heat capacity) and nonreversing (kinetic) thermal events. (3)

Heat capacity, Cp, and changes in Cp, may be calculated using this component. Finally, *f*(T,t) corresponds to the kinetic (nonreversing) heat flow component and is calculated by subtracting the heat capacity component from the total heat flow.

Example MDSC data is shown in figure 1.1.4 corresponding to a quench cooled sample of a mixture of polyethylene terephthalate (PET) and polycarbonate (PC).(3) Note that the total heat flow (central green trace), similar to a traditional DSC analysis, cannot distinguish between the cold crystallization of PET and the T_g of PC. However, the reversing component of the total heat flow (bottom blue trace) clearly reveals T_g of PC and melting of PET.

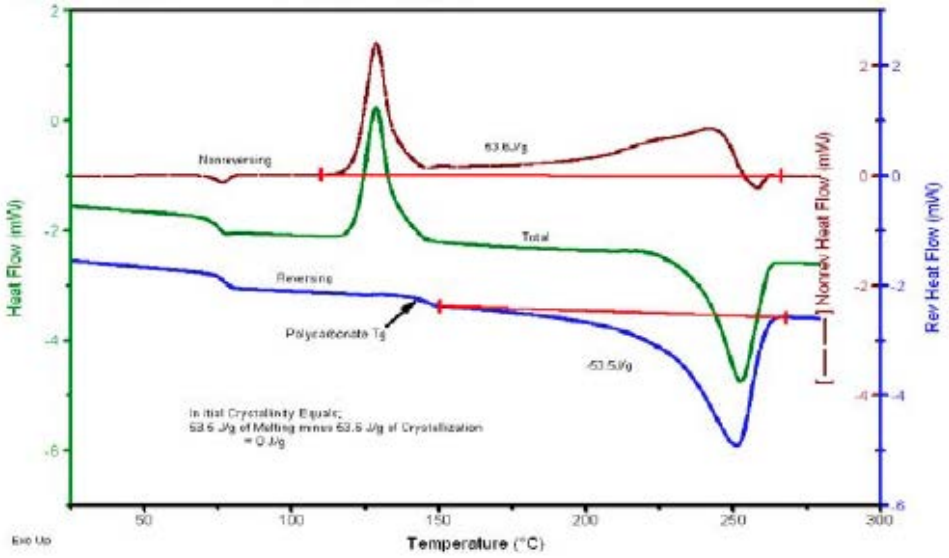

Figure 1.1.4: Example MDSC data corresponding to a quench-cooled mixture of polyethylene terephthalate (PET) and polycarbonate (PC). Nonreversing heat flow is shown in red, total heat flow (similar to standard DSC) is shown in green, and reversing heat flow is shown in blue. (3)

These data clearly illustrate the advantages of MDSC over standard DSC for deconvolution of the thermal behavior of multicomponent samples (commonly encountered in both synthetic and biological materials). MDSC also enhances sensitivity when observing weak transitions such as those seen in some liquid crystalline phase transitions. Additionally, MDSC simultaneously improves measurement resolution, enabling separation of closely spaced thermal transitions, such as those that will most likely be observed in quasi-crystalline anisotropic nanomaterials (e.g., optical metamaterials).

1.1.2 Discovery Series DSC System Components: The Discovery Series DSC (part # 972000.901) was purchased as a DSC/TGA (see section 1.2) combination that operates from the Discovery Common Cabinet (part # 922000.901) with a built-in user interface in addition to the required control computer (part # 924500.901).

Purchase of the Discovery Series DSC included: a self-calibrating 50-position auto-sampler, gas delivery module, TA Instruments patented Modulated DSC technology, and Trios software. The Trios software allows for complete instrument control, data logging, and data analysis.

Purchase of the Discovery Series DSC also required the purchase of a refrigerated cooling system for best operating performance. The cooling system purchased was the Discovery Refrigerated Cooling System – RCS90 (part # 972007.901). The RCS90 consists of a two-stage cascade vapor compression refrigeration apparatus and allows for a programmed or ballistic cooling from -90 °C to 550 °C.

Miscellaneous required items and consumables purchased included: Tzero™ Press and Die Sets Kit (part # 901600.901) and RCS Gas Drying Tube (part # 200266.001).

Total Cost (DSC & TGA): The standard purchase price for the DSC plus TGA system (see also section 1.2) is $224, 155.00. However, TA Instruments has extended a "Buy 1 Get 1 Free" offer for the lesser value item. The total discount was - $92,600.00, reducing the system total to $131,555.00

1.2. Thermogravimetric Analyzer (TGA). Thermogravimetric analysis assesses the change in the mass of a bulk material sample, placed in a controlled atmosphere, as a function of temperature and/or time. Analogous to DSC analysis, a sample of known mass is subjected to a programed temperature ramp (either heating or cooling) while subjected to a chosen atmosphere. This atmosphere may be reactive or inert. Again, similar to DSC, a change in the sample that occurs at a specific temperature reveals information about thermally controlled processes. In the case of TGA analysis, the sample under test either gains or loses mass while being heated or cooled at a controlled rate, in a controlled environment. TGA analysis, using a thermogravimetric analyzer, is commonly employed to quantify nanoparticle purity, nanoparticle coating percentage,(4-6) loss of solvent (e.g., degree of hydration/residual solvent), sample composition, decomposition temperature, oxidation kinetics, and others.

1.2.1 Instrument Overview: TA Instruments Discovery Series TGA. Similar to the Discovery Series DSC, The Discovery Series TGA (figure 1.2.1) from TA instruments provides best-available performance. A number of innovations (proprietary to TA Instruments) are combined to deliver the industry leading performance that makes the Discovery Series TGA the top choice for highly accurate and sensitive thermogravimetric analysis. Each component of The Discovery Series TGA has been designed with the "System" in mind. A proprietary vertical balance design in which the mechanical components and measurement electronics are thermally isolated allows

for very high stability and accuracy in mass measurement. This thermal isolation is essential for maintaining baseline flatness while the temperature of the furnace and sample are varied from ambient to 1200 °C at a potentially very high rate of change (figure 1.2.1, right). The discovery TGA furnace design employs a silicon carbide (SiC) inner chamber. Four halogen lamps surrounded by a water-cooled jacket allow precise temperature control for linear heating rates from 0.1 to 500 °C/min, or ~ 2000 °C/min ballistic heating. In order to precisely control the measurement atmosphere, TA Instruments has implemented a high-performance horizontally oriented gas delivery system. Gas flow introduced perpendicularly to the sample chamber and very close to the sample under test ensures minimum noise introduction and fast, complete, atmosphere change when gas mixtures are switched abruptly. The gas delivery system that is included as standard equipment with the Discovery Series TGA allows for mixing any

Figure 1.2.1: The Discovery Series TGA System (left). Cutaway diagram of the Discovery Series TGA IR furnace (right). The water cooled jacket, furnace interior and horizontal gas delivery system are shown. (3)

desired ratio of two chosen reactive or nonreactive gasses (e.g., nitrogen or oxygen).

The improvements outlined above (improved balance sensitivity and stability, highly controllable furnace, and improved gas introduction) enable the use of TA Instruments' patented HI-Res™ TGA furnace control algorithms. HI-Res™ TGA employs a dynamic heating rate to maximize weight change resolution. In essence, high heating rates are used when no change is occurring and the heating rate is slowed dramatically as thermal transitions are detected. This method allows for high resolution while maintaining short measurement times (figure 1.2.2). Additionally, combined high sensitivity and resolution allow analysis of complex samples that display multiple thermally activated changes with similar thermal activation energies.

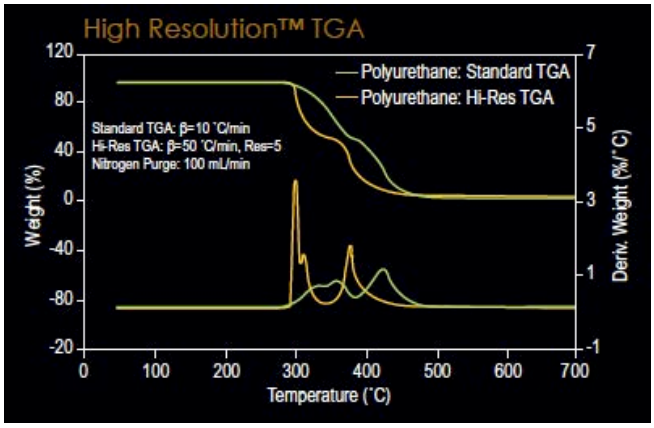

Figure 1.2.2: Demonstration of the resolution improvements seen using the HI-Res™ TGA technique as compared to standard linear heating rate analysis.(3)

In addition to HI-Res™ TGA, the Discovery Series TGA is also equipped with modulated TGA (MTGA) capability as a standard feature. MTGA is similar in operating principle to the MDSC technique outlined in section 1.1.1. MTGA combines a linear ramp rate (or in this case HI-Res™ TGA method) with a sinusoidal thermal modulation. The use of a discrete Fourier transformation data analysis algorithm allows continuous analysis of activation energies for thermal events as a function of time and temperature.

1.2.2 Discovery Series TGA System Components: The Discovery Series TGA (part # 954000.901) was purchased as a DSC/TGA (see section 1.2) combination that operates from the Discovery Common Cabinet (part # 922000.901: also listed in section 1.1.1) with a built-in user interface in addition to the required control computer (part # 924500.901: also listed in section 1.1.1).

Purchase of the Discovery Series TGA included: a self-calibrating 25-position auto-sampler with a sealed-pan punching system, an integrated electromagnet for automated thermal calibration, gas delivery module, TA Instruments' patented HI-Res™ TGA and Modulated TGA technology, and Trios software.

A Discovery Dual Module Upgrade Kit (part # 922303.901), and a DSL Router with 4-Port Switch (part # 251471.002) was required for simultaneous operation of the Discovery DSC and TGA using the Discovery Common Cabinet and control computer (also purchased with the funds awarded here).

Total Cost (DSC & TGA): As outlined in section 1.1.1, several items (i.e., part numbers: 922000.901, 924500.901, 922303.901) are used in common when the DSC/TGA instrument combination is purchased.

The quoted price for the DSC plus TGA system (see also section 1.1) is $224,155.00. However, TA Instruments has extended a "Buy 1 Get 1 Free" offer for the lesser value item. The total discount was be - $92,600.00, reducing the system total to $131,555.00

1.3. Polarized Light Microscope (PLM). Polarized light microscopy is an optical contrast enhancement technique that allows quantitative analysis of anisotropic materials.(7) The PLM method is widely used by materials scientists, geologists, and biologists in the study of, for example, liquid crystals, crystallography, and anisotropic sub-cellular assemblies. PLM combines high sensitivity and ease of use with the ability to gather large or small area quantitative images. In essence, a microscope is equipped with two polarizers placed in the optical path. The first polarizer sets the polarization state of the incident light. The second polarizer (also called the analyzer), placed after the sample under test, is set to minimize transmitted or reflected light intensity, as detected by eye, camera, spectrometer, etc. (i.e., the polarizers are crossed). A birefringent sample unequally retards incident surface- and plane-polarized light waves, shifting the initial polarization state (vector sum of electric fields). This shift in polarization state results in a light intensity increase (transmitted through the analyzer) at the detector.

In the case of monochromatic light, the intensity at the detector may be simply described using.

$$T = \sin^2\left(\frac{\delta}{2}\right) \qquad \delta(V,T,\lambda) = \frac{2\pi d\Delta n(V,T,\lambda)}{\lambda} \qquad (1.3.1)$$

Here, relative transmittance, T, is related to the induced phase retardation, δ, which can be used to solve for birefringence, Δn, when the light wavelength, λ, and sample thickness, d, are known.

As the sample is rotated, or the crystal axis orientation is altered by other external means (e.g., electric field application) birefringence effects may be easily monitored.

In practice, PLM is a white-light imaging technique, making analysis more complicated than is suggested by the simple illustration of principle above. However, imaging allows extraction of a wealth of additional (e.g., spatial and color) information from a single experiment.(8) For example, nonuniform isotropic samples may display spatially dependent optical properties and/or exhibit other phenomena such as pleochromic effects (variations in absorption spectrum with respect to light polarization direction). Such effects may be used to gather information about spatial variations in optical propagation constants using e.g., Michel-Levy color analysis. With the addition of a Bertrand lens, and various retardation (compensator) plates, conoscopic interference patterns may also be observed and analyzed.

1.3.1 Instrument Overview: Olympus BX51 Polarized Light Microscope System. The Olympus BX51 PLM system (figure 1.3.1) provides industry-leading performance. The Olympus BX51 Light Microscope system requested here is configured specifically for use in Polarized Light Microscopy (PLM) applications. However, it is a modular microscopy system, and can therefore be easily reconfigured to fulfill a variety of optical microscopy research needs.

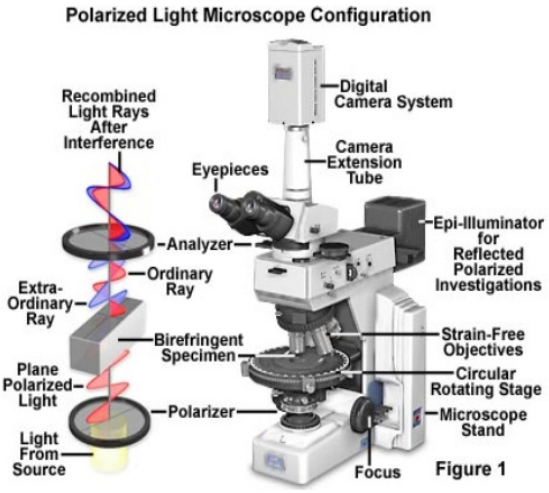

Figure 1.3.1: A schematic of the Olympus BX51 Polarized Light Microscope system. The BX51 body is capable of transmittance and reflection (epi) illumination. The system is equipped with: two 100-Watt halogen illumination lamps; the appropriate polarization optics; strain-free objectives; a rotation stage, a Bertrand lens; and a digital camera with spectrometer adapter.

Following purchase, this system has been interfaced with existing equipment in the Sullivan Lab at MSU (e.g., polarized absorption spectroscopy, single-beam ellipsometry). The anisotropy data collected using PLM will serve to directly complement larger area and single-wavelength ellipsometry measurements by adding white-light spectroscopic imaging, and small-area probing capabilities. This BX51 PLM system is equipped with: two 100-Watt halogen lamps (one for epi illumination); a polarizer and rotatable analyzer combination; high-quality strain-free objectives to allow for undistorted collection of polarized light; a rotation/translation stage so that the sample may be investigated as the optical axis is rotated; a Bertrand lens for conoscopic (interference) imaging; a digital camera system and the appropriate mount for attachment of a fiber-coupled CCD spectrometer (Ocean Optics).

1.3.2 Olympus BX51 PLM System Components: All system components are assembled onto a basic Olympus BX51TRF-6 microscope frame with two lamp sockets (part # BX51TRF-6). Transmission and epi illumination lamps are first added (part # 5-UL1227 and 8-C406). Epi illumination also requires a second lamphouse (part # 5-UL1237) and a reflected light illuminator (part # 5-UR720) (purchased here). Next, a swing-out strain free rotatable polarizing condenser is introduced into the light path (part # 6-U310). Above the condenser, the sample is held by a

circular rotating centerable stage (part # 4-U355) with mechanical X-Y translation controls (part # 4-U390). The objectives are held by a polarizing quadruple nosepiece (part # U-R164) attached to the microscope head assembly. The head assembly also houses: the rotatable analyzer (part # U-P520); Bertrand lens for conoscopic viewing (part # U-P515); an adapter for compensator plates (part # U-P530); and a trinocular observation tube for attachment of eyepieces, camera, and spectrometer accessories (part # 3-U234). The DP73-1-51 digital camera (part # 7-D773-51) is attached using a C-mount adapter (part # U-V111C) equipped with a side camera port (part # U-IT134EC) for simultaneous fiber-coupled spectrometer operation. Required optics included: two eyepieces (part # 2-U1026 and 2-U1007); four plan fluorite strain free objectives (10X, 20X, 40X and 100X-oil, part # 1-U2D523, 1-U2D525, 1-U2D527, and 1-U2D535); and four quantitative analysis compensators (full-wave gypsum, quarter-wave mica, 1-4 lambda quartz wedge, and 1 lambd, part # U-P521, U-P522, U-P546, and U-P540). Miscellaneous required parts include: Cellsens standard imaging analysis software (part # CS-ST); US three-prong power cord (part # UYCP-11); and microscope dust cover (part # OMT-010).

Total Cost: The purchase price for the complete Olympus BX51 PLM system as outlined above was $37,248.00. This equipment was purchased and installed with the funds provided here.

2. Impact on Metamaterials Research and Research-Related Education

In addition to the metamaterials program (Sullivan ARO # W911NF-12-1-0333) discussed below, the purchase of the equipment purchased here is also benefiting the ONR MURI (grant # N00014-10-1-0946) currently funded to explore the biocorrosion of carbon steel and fuels. This point is discussed further in section 3.

2.1 Impact of Thermal Analysis and Polarized Light Microscopy Equipment on Nonlinear Metamaterials Research. Metamaterials are artificial media constructed from arrays of sub-wavelength, polarizable elements. Optical metamaterial technologies, often consisting of 2- or 3-dimensional arrays of ordered metallic nanoparticles, offer new and uniquely valuable properties, many of which are extremely difficult or impossible to achieve with natural materials. Examples include materials for communications and sensing, sub-wavelength imaging, superlensing (visible, IR, terahertz),(9, 10) filtering, and field enhancement.(11-13) In addition to the construction of improved static EM media, many applications envisioned require the development of active (dynamically reconfigurable) metamaterials. The introduction of tunability or dynamic response into materials such as photonic bandgap or negative index materials (NIMs) would enable optical information processing (active optical switches, filters, memory elements), compact beam steering, optical frequency conversion, imaging, and other technologies.

Nonlinear optical metamaterials (NLMMs), or metamaterials hybridized with nonlinear optical media, offer a route to both efficient and high-speed tuning in a variety of functions. In NLMMs, the magnitude of observed nonlinear effects depends on the nonlinearities of the constituent elements, as well as the structurally-induced focalization of incident (electric) fields. Thus, the efficiency of the desired nonlinear processes can be maximized on two fronts: first, by enhancing the nonlinearity of the materials used, and second, by optimizing the design of metamaterial architectures to provide maximum electric field enhancement.(12) In contrast to plasmonics, however, metamaterial concepts allow homogenization over large, periodic arrays of sub-wavelength field concentrations, achieving enhanced bulk (continuous) effective nonlinear properties. In addition, these same concepts enable fine control over susceptibility tensor element orientation. These features distinguish NLMMs from simple plasmonic and resonant E-field enhancement strategies. For these reasons, resonant and nonresonant metamaterial architectures represent an ideal platform with which to exploit the ultrafast E-field induced $\Delta\varepsilon$ offered by second (Pockels, $\chi^{(2)}$) and third order (Kerr, $\chi^{(3)}$) organic nonlinear optical materials (ONLOs).

ONLOs can deliver second-order nonlinear optical coefficients that are larger by more than an order of magnitude than those of $LiNbO_3$, or other similar inorganic materials.(14-16) Such hybrid integration of highly-active ONLOs within optimized metamaterial structures promises to yield NLMMs capable of optical parametric amplification,(13, 17) self-phase modulation (18, 19), and new nonlinear phenomena such as the nonlinear optical mirror,(20) and the mirrorless optical parametric oscillator/amplifier, shown schematically in figure 2.1.1b.(11-13, 17, 21, 22)

A DoD (Army Research Office Grant # W911NF-12-1-0333) funded program entitled "Amphiphilic Block Copolymer Mediated Self-Assembly of Nanocomponents Into Active Metamaterial Structures: Nonlinear Metamaterials" is currently underway in the research labs of Philip A. Sullivan, at Montana State University, and David R. Smith, at Duke University.

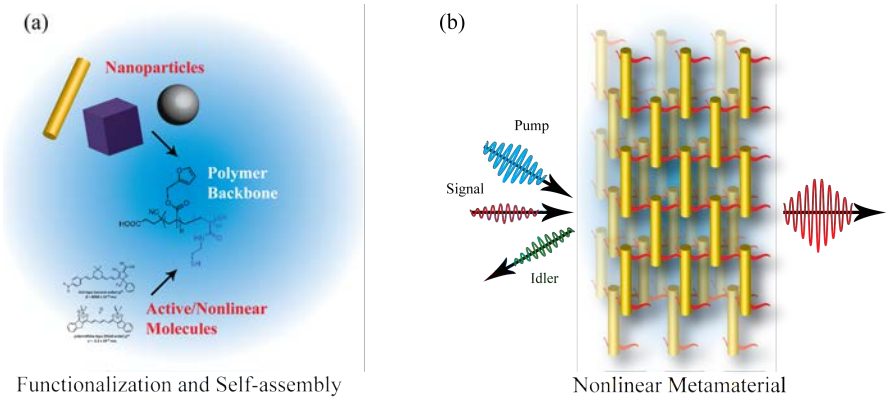

Figure 2.1.1: (a) Idealized schematic of the self-assembly technique for constructing NLMMs. Carefully designed nanoparticles are integrated structurally along with active and nonlinear molecules, joined through a polymer "backbone" to form a self-assembling pseudo tri-block (A-B-A) copolymer. (b) Illustration of a self-assembled "cut-wire" NLMM employed as a mirrorless optical parametric amplifier. Note that, in this metamaterial, the idler wave propagates counter to the pump and signal waves, providing a natural mechanism for feedback.(4)

In this program, NLMMs consisting of periodic arrays of nanoparticles are being prepared by using specially designed organic materials to simultaneously mediate self-assembly and introduce large nonlinearities. Amphiphilic or (otherwise appropriately functionalized), block copolymers are used to concurrently control element organization and serve as scaffolds for the incorporation of highly active organic nonlinear optical (ONLO) chromophores.

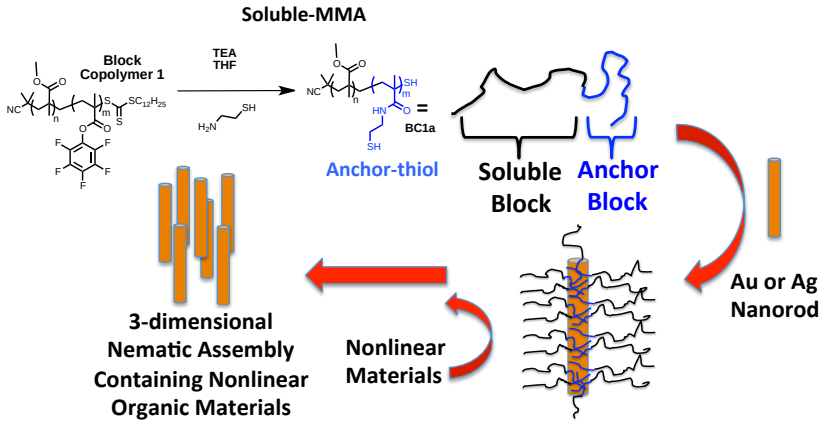

Scheme 2.1.1: RAFT polymerization and post- functionalization of proposed diblock copolymer 1 (DBP-1). DBP-1 is attached to a gold or silver nanorod, and cast onto a substrate. Solvent and thermal annealing

provide nematic-like order. Nonlinear materials may be dispersed within the polymer matrix, covalently attached to either block, or associated with the nanoparticle.

Asymmetries derived from high length/width aspect ratio nanoparticles, coupled with the disparate properties of dissimilar polymer blocks, are being harnessed to realize truly "bulk" materials with engineered long-range nanoscale structure (figure 2.1.1). Such hybrid integration not only allows the metamaterial to assume the nonlinearities of the ONLO medium, but is also predicted to yield significantly enhanced bulk nonlinear susceptibilities.(12, 23) Unlike conventional plasmonic and resonant cavity devices, the metamaterial concept distributes regions of field enhancement periodically throughout the bulk medium, yielding optically homogeneous materials with designer anisotropy and dispersion characteristics, as well as greatly enhanced nonlinear susceptibilities.

Nanoscale element mobility transitions (melting or glass transition) are to be tuned by design to optimize thermal annealing and enable E-field control over nanocomponent and susceptibility tensor element orientation.

2.1.1 Impact of Thermal Analysis Equipment (TA Instruments Discovery Series DSC and TGA): Tuning of polymer, small molecule and liquid crystal phase transition temperatures (e.g. glass transition, T_g, melting, T_m, clearing, T_c) via modification of the molecular and/or macromolecular structure is essential for optimizing processibility and function. In the case of organic second-order nonlinear optical (electro-optic) materials, such as those to be incorporated here, acentric molecular order is most commonly induced through a process known as electric field poling. In essence, the initially isotropic material is heated to near T_g (thermal annealing) and then cooled under the application of a powerful external DC electric field.(24) Upon heating to near T_g, enough thermal energy becomes available to increase molecular reorientation rates by up to 11 orders of magnitude. Dipolar, nonlinear optically active, subunits (chromophores) are then able to translate and/or rotate. Interaction between the permanent dipole moments of the chromophores and the electric poling field induces enough unidirectional molecular order to break symmetry and induce second-order nonlinear optical behavior. Similarly, molecular (and corresponding director axis) orientation in various liquid crystalline phases may be controlled by the application of an external electric field. However, in the case of liquid crystalline materials, a permanent molecular dipole moment is not required. Instead, an induced dipolar response allows the liquid crystal lattice to be deformed by an applied electric field in what is known as the Freedericksz transition.(25) This mechanism allows liquid crystals to be oriented in two dimensions using AC and/or DC electric fields. Analogous to organic electro-optic materials, thermotropic liquid crystals exhibit thermally induced solid/liquid and order/disorder transitions across relatively narrow temperature ranges.

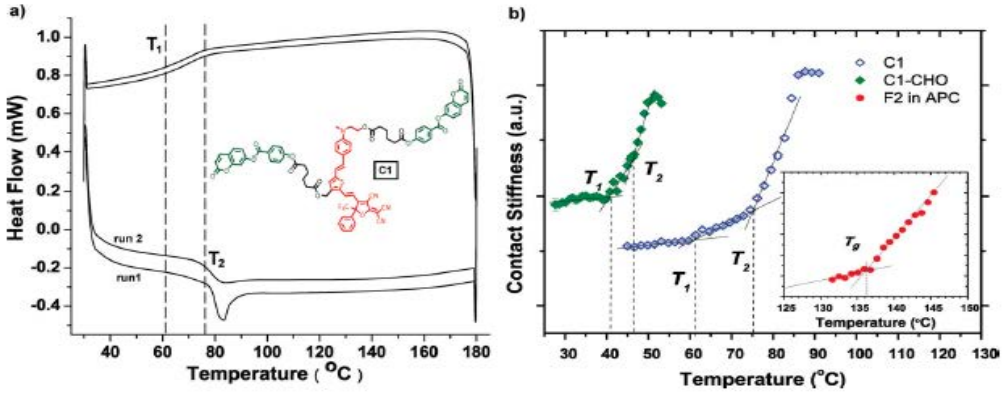

Figure 2.1.2: a) DSC analysis measured for C1. **b)** Complimentary Shear Modulation Force Microscopy (SMFM) analysis of C1 and relevant control compounds. Thermal analysis of C1 clearly shows two distinct transition temperatures: T_1 and T_2.(26, 27)

In order to fabricate and control anisotropic hybrid organic/metal nanoparticle arrays such as those illustrated above (figure 2.1.1 and 2.1.2) application of AC and/or DC fields at the appropriate time and temperature will be used to precisely control order. Both dipolar and liquid crystalline (nematic-like) behavior is expected in these hybrid materials.(5) AC fields will be used to control centric order ($\cos^2\theta$), as in the case of metal nanorods, and DC fields will be used to induce acentric order ($\cos^3\theta$), as in the case of dipolar small-molecules. Precise thermal control will allow activation or suppression of molecular or nanocomponent mobility transitions.

Figure 2.1.2 shows thermal analysis data for the pendant modified organic electro-optic material C1.(26, 27) A DSC trace corresponding to C1 is shown at the left (**a**) and complimentary data from shear modulation force microscopy (SMFM) analysis is shown on the right (**b**). For comparison, SMFM data corresponding to polymeric (F2 in APC) and reduced dipole (C1-CHO) control compounds are also shown. These data reveal the existence of two distinct thermal transitions corresponding to the activation of separate subunit reorientation. Pendant mobility (subunit shown in green) is activated at a slightly lower temperature than chromophore core (subunit shown in red) mobility due to differences in intermolecular interaction energies. Similar behavior may be expected in the case of the hybrid organic block-copolymer/metal nanorod assemblies currently being prepared. In fact, dissimilarities in size and composition between organic chromophores and metal nanoparticles promise even greater differences in subunit reorientation activation energies. Mobility and phase transition temperatures will be highly dependent on the identity and molecular weight of the block copolymer employed, and the degree of particle functionalization. The quality of the polymer coating will determine the effectiveness of this strategy in controlling nanoparticle aggregation, and enabling ordered phase formation. The highly sensitive Discovery Series DSC purchased here allows detailed investigation of such complicated thermal behavior by employing such capabilities as modulated DSC analysis (section 1.1.1). These investigations are allowing insight into, and optimization of thermal properties. Likewise, the Discovery Series TGA purchased here enables detailed investigation of nanoparticle functionalization (e.g., number of polymer chains per particle) with respect to polymer properties.

2.1.2 Impact of Polarized Light Microscopy System: Anisotropic materials are generally characterized by birefringence (dependence of refractive index on incidence angle and polarization) and dichroism (dependence of optical absorption on incidence angle and polarization).

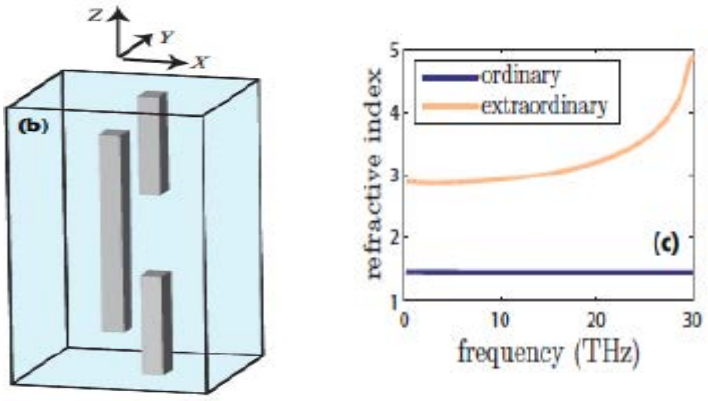

Figure 2.1.3: Simulation results for overlapping metallic bars (left) embedded in a dielectric medium. n_o and n_e are expected to display a nearly three-fold difference (right).

The oriented nanorod lattice currently being prepared (section 2.1) is predicted (full-wave computer simulations) to display large optical anisotropy, as indicated by the nearly three-fold difference in ordinary and extraordinary refractive indices shown in figure 2.1.3.(12) As such, the speed of the extraordinary wave relative to the ordinary wave can be tuned over a massive range by simply rotating the direction of propagation relative to the metamaterial's director axis. Physical sample rotation and/or externally applied control fields, may be used to reconfigure this orientation. This control translates directly to the efficiency of nonlinear phenomena for a wide range of configurations and frequencies. Polarized light microscopy will allow quantitative investigation of both birefringent and dichroic properties of these materials. Dichroism measurements may be directly used to quantify the order of individual subunits according to equation 2.1.1.(28-30) Here A-parallel and A-perpendicular represent the absorption of light polarized parallel and perpendicular to the molecular and/or nanocomponent orientation axis.

$$S = \frac{A_{ll} - A_{\perp}}{A_{ll} + 2A_{\perp}} \quad S = \langle P_2 \rangle = \frac{1}{2}\left(3\langle \cos^2\theta \rangle - 1\right) \qquad (2.1.1)$$

In the case of organic nonlinear optical chromophores, dichroism arises from the selective electronic absorption of polarized light by colored organic molecules having transition dipole moments oriented parallel to the electric field of the incident light.(28) Likewise, the anisotropic absorption of polarized light by metallic nanorods arises from selective interaction of the transverse (A-perpendicular) or longitudinal (A-parallel) surface plasmon with the electric field of the incident light.(29)

Because PLM is a white-light imaging technique, simultaneous spatial and intensity measurements provide a wealth of information about the uniformity of the sample under test. Additionally, when coupled with a spectrometer, simultaneous order measurements may be obtained corresponding to individual material subcomponents with distinct absorption characteristics.(26)

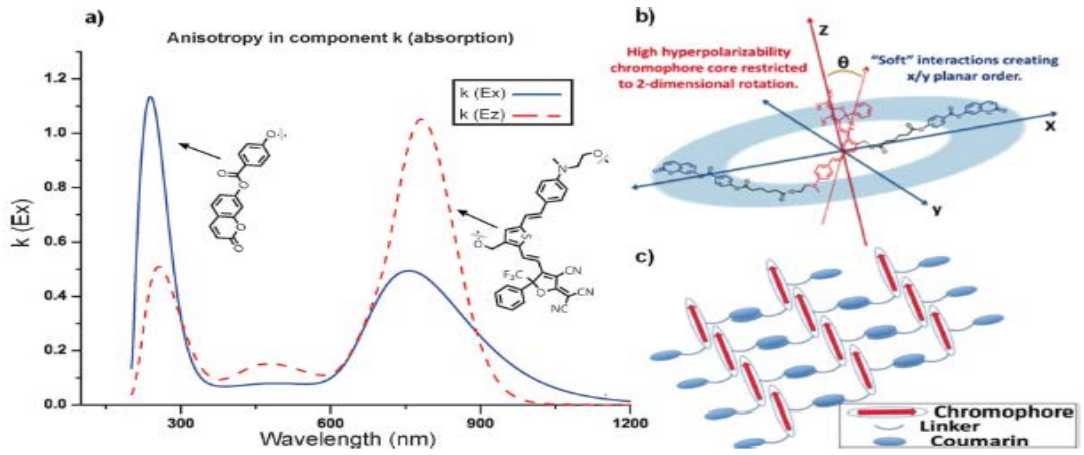

Figure 2.1.4: a) The k components of the refractive indices as a function of wavelength for the x- and z-planes are shown for the organic electro-optic material C1, illustrating the unique absorptions and orthogonal orientations of the coumarin-pendant and chromophore subunits. b) The relative orientations of chromophores (xz, yz planes) and the coumarin pendant groups (x-y plane) are shown. c) A cartoon illustrating the bulk coumarin orientations present in an inter-coumarin network in the plane orthogonal to the poling axis.

To illustrate this point, an example is again taken from recent work by Sullivan, Dalton, and Robinson et al. Figure 2.1.4 illustrates such an analysis that was performed on the organic electro-optic material C1.(26) When investigated using spectroscopic ellipsometry, it was revealed that after being oriented under the influence of a DC poling field, the individual molecular subunits in C1 were oriented perpendicular to one another. This conclusion was supported by order determinations using anisotropies in the imaginary (absorptive) component of the complex refractive index, k. Similar analysis may be performed on hybrid NLMMs using spectroscopic polarized light microscopy, implementing the Olympus BX51 PLM system purchased here. Because NLMMs are composed of ordered metallic nanocomponents interspersed with organic nonlinear optical materials, the ability to measure the degree of order for both components is critical to the success of the program.

2.1.3 Impact on Advanced Scientific Education: Dr. Sullivan has mentored or co-mentored many talented graduate, undergraduate and post-doctoral students in the laboratory setting. Previously at UW, he co-mentored a number of excellent undergraduates from diverse socioeconomic backgrounds through an REU exchange program, funded by NSF (in connection with the Science and Technology Center, CMDITR). Several of these undergraduates have contributed to peer reviewed publications, and continued on into graduate studies at schools such as Harvard and Northwestern University. At MSU, Professor Sullivan seeks to enhance multi-university, interdisciplinary research opportunities for undergraduate and graduate students alike. Undergraduates are currently recruited to participate in research and supported in collaboration with the McNair Scholars program at MSU. Emphasis is directed toward: first in family to attend college, low-income, and/or members of minority groups. These students are currently participating in this DoD funded research program, alongside students from collaborating groups and Universities (University of Washington, Duke University). Inter-institution communication is facilitated by videoconferencing capabilities as well as inter-site travel. In addition to laboratory mentoring, Dr. Sullivan is currently working with the departmental administration to support the development of a special topics course that will cover the design, synthesis and application of organic photonic materials. This course will be available to both graduate and undergraduate

majors and will help to broaden the exposure of students to interdisciplinary materials and photonics related research.

The equipment purchased here serves to broaden student access to state-of-the-art materials science research instrumentation. Both the thermal analysis equipment and the PLM system add significant breadth and depth to the materials science capabilities previously in place at Montana State University. This enhances research competencies on campus and broaden student exposure and understanding in a wide variety of fundamental research areas.

3. Institutional Impact: Importance to Ongoing Research of Interest to DoD

3.1 Overlapping Uses and Impact on Ongoing Research at MSU: Previous to the purchase of this equipment, Montana State University, Bozeman, did not own thermal and optical materials analysis equipment with comparable capabilities. The instruments purchased here fill a much-needed void. MSU is otherwise very well equipped to pursue cutting edge research in a large number of disciplines. For example, the Chemistry and Biochemistry Department houses three state-of-the art shared facilities: the mass-spectrometry (Mass-Spec) facility, the NMR and X-ray facility: http://www.chemistry.montana.edu/facilities/ and the Center for Bioinspired Nanomaterials (CBIN) and the Transmission Electron Microscope Facility (TEM): http://caffeine.chemistry.montana.edu/~tdouglas/nano/. The Mass-spec facility houses six mass spectrometers including ESI-TOF and MALDI-TOF. The NMR and X-ray facility contains four NMR spectrometers, a Bruker DRX250, DPX300, DRX500, and a Bruker DRX600. The X-ray facility includes a four-circle automated diffractometer. The TEM facility houses a LEO 912 AB TEM., and the CBIN houses both dynamic and multi-angle light scattering instruments. In addition, the MSU physics and engineering departments house the Montana Microfabrication facility (two-cleanrooms with CMOS fabrication capabilities: http://www.mmf.montana.edu/), and the Imaging and Chemical Analysis facility (ICAL). ICAL houses a suite of instruments for sample characterization through microscopy and spectroscopy. Two atomic and magnetic force microscopes from Veeco, a field emission scanning electron microscope, a scanning electron microscope, a scanning Auger microprobe, a powder X-ray diffraction system equipped with a thin film attachment, a time-of-flight secondary ion mass spectrometer, and an X-ray photoelectron spectrometer equipped with standard and monochromatized X-ray sources. In complement to the equipment and capabilities discussed above the thermal analysis equipment and the PLM system purchased here significantly augment materials characterization capabilities of interest to DoD at MSU.

3.1.1 High-temperature and Bio-corrosion research: Professor Paul Gannon (MSU Chemical and Biological Engineering Department, and director: MSU High-Temperature Materials Laboratory) and others are currently exploring high-temperature corrosion and corrosion reduction (see letter attached). This research is of primary interest for protection of materials used in turbine engines, and similar systems. The DSC/TGA systems purchased with the funds provided are capable of simulating high-temperature combustion environments, while precisely measuring test specimen mass and indicating critical phase changes as a function of environmental exposure. In this way, DSC and TGA are being employed to characterize the oxidation (corrosion) rates of various metal alloys and ceramics used in combustion systems, as well as evaluate the efficacy of protective surface coatings.(31)

Professor Steven Sophie, an assistant professor of the MSU Department of Mechanical and Industrial Engineering, is developing new anode technologies for high-temperature electro-chemical power generation as well as high-temperature electrolysis. Two approaches to high temperature stability are the fabrication of mixed conducting double perovskite materials as well as the thermal stabilization of the nickel catalyst nano-particles. New double perovskites being

synthesized at MSU need to be characterized for chemical and structural uniformity, and thermal properties. Composition drift can induce secondary phase formation at very small scales and at surfaces exposed to reducing gases that can shift both electronic and oxygen ion conduction characteristics, embodied as degradation of the anode phase. Further, stabilization of nickel nano-catalysts has been achieved in cermets through secondary phase meta-stable chemical additives. Decomposition of the additives facilitates a stepwise chemical interaction with the metal and ceramic phase creating a chemical anchor to prevent metal coarsening.

MSU engineering is also currently funded by an ONR MURI (grant # N00014-10-1-0946) to explore the biocorrosion of carbon steel and fuels that are exposed to seawater. The goal of this research is to predict, diagnose and mitigate fuel biodeterioration and biocorrosion problems impacting US Navy operations.

3.1.2 Assessing The Thermal Characteristics of Polymers Encapsulated Within the P22 Bacteriophage Capsid: The research group of Professor Trevor Douglas (Director: MSU Center for Bioinspired Nanomaterials) has pioneered the use of viruses as supramolecular platforms for synthetic manipulation with a range of applications from materials to medicine (see letter attached).(32, 33) Through understanding of the inherent properties of these viral capsid architectures, which include high symmetry and self-assembly, they can be rationally exploited as synthetic templates. An appreciation of these properties has resulted in a paradigm shift from the study of viruses as purely disease causing agents to highly useful supramolecular assemblies, which can be chemically and genetically modified.

The Douglas group has shown that the formation of polymer networks, on the inside of these protein cage nanoparticles significantly changes the physical properties of the protein-polymer composite. Understanding these properties, and how they change, is fundamental to exploiting them for a wide range of applications. Recent work has shown that the P22 bacteriophage capsid can be used to initiate polymer growth using either [3+2] azide-alkyne cycloaddition or atom transfer radical polymerization reactions. These internally constrained (and crosslinked) polymers increase the functional internal surface area of the capsid by an order of magnitude or more. The polymers can be functionalized with Gd-chelates, making these modified capsids extremely efficient magnetic resonance imaging contrast agents(34).

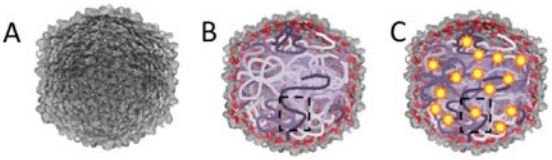

Figure 3.1.1 The bacteriophage P22 capsid. (A) cryoTEM model of the recombinant virus like particle (VLP) of P22 (B) the P22 VLP with an encapsulated ATRP polymer, (C) internal ATRP polymer labeled with imaging agent (fluorescence or MRI.

In addition, the crosslinked polymers change the thermal stability and stiffness of the capsid considerably. Single particle deformation experiments with polymerized capsids show that the stiffness of the capsid doubles upon polymerization.

Also, the thermal stability of the capsid is also dramatically altered upon internal polymerization. These protein cage capsids are assembled from tens or hundreds of identical protein subunits. Upon heating, they lose quaternary structures and the cages disassemble and fall apart and the subunit proteins denature and aggregate irreversibly. However, when internally polymerized, the cages are able to withstand hydrothermal (120ºC) bomb reactor conditions without protein loss(35, 36). Since the polymers are covalently attached to the interior of the capsid, and the degree of crosslinking can be controlled, these systems might act in manner analagous to that described by Don Ingber as molecular tensegrity where internal elastic forces can accommodate deformation of the structure (37) without catastrophic disassembly. A wide range of different polymers have now been synthesized inside these protein cage architectures including (*N*-isopropylacrylamide) polymers that are thermally responsive, coordination polymers(38, 39) that are crosslinked (via metal chelation), click(35, 36, 40), and ATRP polymers (acrylamide and acrylate) (39). Our goal is to characterize the physical properties of these protein-polymer

composites using differential scanning calorimetry to probe structural transitions in both the protein cage architecture, the material encapsulated within the capsid, and the composite. The TA instruments DSC and TGA system purchased here will play an integral role in these studies.

Bibliography:

1. TAinstruments (2012) www.tainstruments.com.
2. Skoog, D. A., Holler, F. A., Nieman, T. (1998) *Principles of Instrumental Analysis* (New York) 5th Ed.
3. O'Neill, M. J., 1964. The Analysis of a Temperature Controlled Scanning Calorimeter. *Anal. Chem.* 36(7), 1238-1245.
4. Zorn, M., Meuer, S., Tahir, M. N., Khalavka, Y., Sönnichsen, C., Tremel, W., Zentel, R., 2008. Liquid crystalline phases from polymer functionalised semiconducting nanorods. *J. Mater. Chem.* 18(25), 3050.
5. Zorn, M., Tahir, M. N., Bergmann, B., Tremel, W., Grigoriadis, C., Floudas, G., Zentel, R., 2010. Orientation and Dynamics of ZnO Nanorod Liquid Crystals in Electric Fields. *Macromol. Rapid Commun.* 31(12), 1101-1107.
6. Zorn, M., Zentel, R., 2008. Liquid Crystalline Orientation of Semiconducting Nanorods in a Semiconducting Matrix. *Macromol. Rapid Commun.* 29(11), 922-927.
7. McCrone, W. C., McCrone, L. B., Delly, J. G. (1978) *Polarized Light Microscopy* (Ann Arbor Science Publishers, Ann Arbor).
8. Massoumian, F., Juskaitis, R., Neil, M. A. A., Wilson, T., 2003. Quantitative polarized light microscopy. *J. Microscopy* 209(1), 13-22.
9. Linden, S., Enkrich, C., Wegener, J., Zhou, J., Koschny, T., Soukoulis, C. M., 2004. Magnetic response of metamaterials at 100 terahertz. *Science* 306, 1351-1353.
10. Shalaev, V. M., Cai, W., Chettiar, U. K., Yuan, H., Sarychev, A. K., Drachev, V. P., Kildishev, A. V., 2005. Negative index of refraction in optical metamaterials. *Optics letters* 30, 3356-3358.
11. Rose A. et al., 2011. Overcoming phase mismatch in nonlinear metamaterials. *Opt. Mater. Express* 1(7), 1232.
12. Rose, A., Smith, D. R., 2011. A quantitaive study of the enhancement of bulk nonlinearities in metamaterials. *Phys. Rev. A* 84, 053805.
13. Popov, A. K., Myslivets, S. A., George, T. F., Shalaev, V. M., 2007. Four-wave mixing, quantum control and compensating losses in doped negative-index photonic metamaterials. *Optics letters* 32, 3044-3046.
14. Sullivan, P., Dalton, L. R., 2009. Theory-Inspired Development of Organic Electro-optic Materials. *Acc. Chem. Res.* 43(1), 10-18.
15. Dalton, L. R., Sulivan, P. A.; Bale, D. H., 2010. Electric Field Poled Organic Electro-Optic Materials: State of the Art and Future Prospects Chem. Rev., 110, 25-55 (2010). *Chem. Rev.* 110.
16. Pereverzev, Y. V., Gunnerson, K. N., Prezhdo, O. V., Sullivan, P. A., Liao, Y., Olbricht, B. C., Akelaitis, A. J. P., Jen, A. K. Y., Dalton, L. R., 2008. Guest-Host

Cooperativity in Organic Materials Greatly Enhances the Nonlinear Optical Response. *J. Phys. Chem. C* 112(11), 4355-4363.
17. Poutrina, E., Larouche, S., Smith, D. R., 2010. Parametric oscillator based on a single-layer resonant metamaterial. *Opt. Commun.* 283(8), 1640-1646.
18. Powell, D. A., Shadrivov, I. V., Kivshar, Y. S., Gorkunov, M., 2007. Self-tuning mechanisms of nonlinear split-ring resonators. *Appl. Phys. Lett.* 91, 144107.
19. Shadrivov, I. V., Kozyrev, A. B., van der Weide, D. W., Kivshar, Y. S., 2008. Nonlinear magnetic metamaterials. *Opt. Express.* 16(25), 20266-20271.
20. Rose, A., Huang, D., Smith, D. R., 2011. Controlling the Second Harmonic in a Phase-Matched Negative-index Metamaterial. *Phys. Rev. Lett.* 107, 063902.
21. Litchinitser, N. M., Shalaev, V. M., 2009. Metamaterials: transforming theory into reality. *JOSA B* 26(12), B161-B169.
22. Canalias, C., Pasiskevicius, V., 2007. Mirrorless optical parametric oscillator. *Nat. Photonics* 1, 459-462.
23. Rose, A., Larouche, S., Huang, D., Poutrina, E., Smith, D., 2010. Nonlinear parameter retrieval from three- and four-wave mixing in metamaterials. *Phys. Rev. E* 82(3), 036608.
24. Dalton, L. R., Sullivan, P. A.; Bale, D. H., 2010. Electric Field Poled Organic Electro-Optic Materials: State of the Art and Future Prospects *Chem. Rev.* 110(1), 25-55.
25. Yang, D.-K., Wu, S.-T. (2006) *Fundamentals of liquid crystal devices* (John Wiley & Sons Ltd, Chichester, West Sussex).
26. Benight, S. J., Knorr, D. B., Johnson, L. E., Sullivan, P. A., Lao, D., Sun, J., Kocherlakota, L. S., Elangovan, A., Robinson, B. H., Overney, R. M., Dalton, L. R., 2012. Nano-Engineering Lattice Dimensionality for a Soft Matter Organic Functional Material. *Adv. Mater.* 24(24), 3263-3268.
27. Benight, S., Johnson, L., Barnes, R., Olbricht, B., Bale, D., Reid, P., Eichinger, B., Dalton, L., Sullivan, P., Robinson, B., 2010. Reduced Dimensionality in Organic Electro-Optic Materials: Theory and Defined Order. *J Phys Chem B*, 25-50.
28. Olbricht, B. C., Sullivan, P. A., Dennis, P. C., Hurst, J. T., Johnson, L. E., Benight, S. J., Davies, J. A., Chen, A., Eichiniger, B. E., Reid, P. J., Dalton, L. R., Robinson, B. H., 2011. Measuring Order in Contact-Poled Electrooptic Materials with Variable-Angle Polarization-Referenced Absorption Spectroscopy (VAPRAS). *J. Phys. Chem. B.* 115, 231-241.
29. Liu, Q., Cui, Y., Gardiner, D., Li, X., He, S., Smalyukh, I. I., 2010. Self-Alignment of Plasmonic Gold-Nanorods in Reconfigurable Anisotropic Fluids for Tunable Bulk Metamaterial Applications. *Nano Lett.* 10(4), 1347-1353.
30. Sullivan, P. A., Dalton, L. R., 2010. Theory-Inspired Development of Organic Electro-Optic Materials. *Acc. Chem. Res.* 43(1), 10-18.
31. Macauley, C., Gannon, P., Diebert, M., White, P., 2010. The influence of pre-treatment on the oxidation beahvior of Co coated SOFC interconnects. *Int. J. Hydrogen Energy* In Press, doi:10.1016/j.ijhydene.2012.1004.1113.
32. Douglas, T., Young, M., 1998. Host-guest encapsulation of materials by assembled virus protein cages. *Nature* 393(6681), 152-155.

33. Douglas, T., Young, M., 2006. Viruses: Making friends with old foes. *Science* 312(5775), 873-875.
34. Lucon, J., Qazi, S., Uchida, M., Bedwell, G. J., LaFrance, B., Prevelige, P. E., Douglas, T., 2012. Use of the interior cavity of the P22 capsid for site-specific initiation of atom-transfer radical polymerization with high-density cargo loading. *Nature Chemistry*, DOI: 10.1038/nchem.1442.
35. Abedin, M. J., Liepold, L., Suci, P., Young, M., Douglas, T., 2009. Synthesis of a Cross-Linked Branched Polymer Network in the Interior of a Protein Cage. *J. Am. Chem. Soc.* 131(12), 4346-4354.
36. Liepold, L. O., Abedin, M. J., Buckhouse, E. D., Frank, J. A., Young, M. J., Douglas, T., 2009. Supramolecular Protein Cage Composite MR Contrast Agents with Extremely Efficient Relaxivity Properties. *Nano Lett.* 9(12), 4520-4526.
37. Ingber, D. E., 1998. The Architecture of Life. *Scientific American* 278, 48-57.
38. Uchida, M., Morris, D. S., Kang, S., Jolley, C. C., Lucon, J., Liepold, L. O., LaFrance, B., Prevelige, P. E., Douglas, T., 2012. Site directed coordination chemistry with P22 virus like particles. *Langmuir* 28, 1998-2006.
39. Lucon, J., Abedin, M. J., Uchida, M., Liepold, L., Jolley, C. C., Young, M., Douglas, T., 2010. A click chemistry based coordination polymer inside small heat shock protein. *Chem. Comm.* 46(2), 264-266.
40. Qazi, S., Liepold, L. O., Abedin, M. J., Frank, J., Prevelige, P., Douglas, T., 2012. Using the Capsid of Bacteriophage P22 for Development of a Highly Efficient MR Contrast Agent. *Molecular Pharmaceutics*, DOI: 10.1021/mp300208g.